CAPILLARY PRESSURE-SATURATION CURVES: TOWARD SIMULATING DYNAMIC EFFECTS WITH THE LATTICE-BOLTZMANN METHOD

MARK L. PORTER[1], MARCEL G. SCHAAP[2] AND DORTHE WILDENSCHILD[1]

[1]Dept. of Geosciences, 104 Wilkinson Hall, Oregon State University, Corvallis, OR 97331
[2]University of California Riverside, Department of Environmental Sciences; George E. Brown Jr. Salinity Laboratory(USDA-ARS) 450 W. Big Springs Road, Riverside, CA, USA

Abstract

The capillary pressure-saturation curve is widely used to characterize hydraulic properties of porous media. It is often assumed that curves measured under equilibrium conditions can be applied to transient flow conditions, and vice versa. However, capillary pressure-saturation curves are not unique. For instance, experimental evidence suggests that capillary pressure-saturation curves exhibit dynamic effects depending on the flow conditions in the the porous system prior to and during the time of measurement. The extent to which dynamic flow conditions affect the measured capillary pressure is currently debated and the exact cause of the observed dynamic effects is not fully understood. In this study a lattice-Boltzmann model was used to simulate dynamic effects in an effort to identify the pore-scale mechanisms responsible for the dynamic effects observed in macro-scale laboratory experiments.

1. INTRODUCTION

Capillary pressure plays an important role in controlling fluid phase configurations for multiphase flow in porous media. At the pore-scale, capillary pressure is defined as the pressure difference between the nonwetting phase fluid and the wetting phase fluid at the interface that separates the two immiscible fluids [Bear, 1972]. The magnitude of the local capillary pressure (i.e. within a single pore) depends upon the radius of the pore, the contact angle and interfacial tension between the two fluids. The most common and practical macro-scale estimate of capillary pressure is based on an empirical relationship that assumes that capillary pressure is a function of saturation of the wetting fluid only [Bear, 1972, Hassanizadeh et al., 2002]. Thus, the macro-scale capillary pressure, P_c, is defined as:

$$P_c = P_n - P_w = f(S) \tag{1}$$

where P_n is the nonwetting phase fluid pressure, P_w is the wetting phase fluid pressure and S is the saturation of the wetting fluid. With this approach the average pressures within each fluid phase are generally measured outside of the porous medium while the system is in a state of equilibrium [Muccino et al., 1998]. This approach assumes that the macro-scale variables (capillary pressure and saturation) uniquely describe the system.

Date: 03/14/2006.

However, this approach does not account for pore-scale properties, such as, fluid-fluid interfacial area, interfacial tension, wettability, geometry of the pore space and contact angle hysteresis, to name a few, that influence the fluid configurations throughout the porous medium.

Experimental and theoretical evidence indicates that these curves are not unique, but depend upon the flow dynamics in the porous system prior to and during the time of measurement (see Schultze et al. [1999], Wildenschild et al. [2001], Hassanizadeh et al. [2002] and references therein). The non-uniqueness of the $P_c - S$ curve due to flow dynamics is generally referred to in the literature as dynamic effects [Wildenschild et al., 2001, Hassanizadeh et al., 2002, O'Carroll et al., 2005]. At the macro-scale, dynamic effects in drainage curves are generally characterized by higher saturations (for a given capillary pressure) than observed in static situations [Topp et al., 1967]. In contrast, during imbibition events higher saturations are measured in the the static curves than in the dynamic curves [Davidson et al., 1966].

Recent advancements in numerical modeling have shown promise for facilitating further investigations of the $P_c - S$ relationship. The lattice-Boltzmann (LB) model has been chosen for this study because it is capable of simulating multi-phase and multi-component fluid flow in complex pore geometries. Various LB models have been applied to multi-phase flow in 3D porous systems [Martys and Chen, 1996, Tölke et al., 2000, Bekri et al., 2001, Vogel et al., 2005, Li et al., 2005]. Pan et al. [2004] has reported a thorough investigation of drainage and imbibition using the SC type model on a reconstructed 3D porous medium. They report simulation results for static $P_c - S$ curves for various porous media and their results compared well with experimental results. To the best of our knowledge, no attempt has been made to use the SC type model to investigate dynamic effects in the $P_c - S$ curve on a 3D porous medium that matches the experimental porous medium.

2. Objectives

An overarching goal of this study is to further investigate dynamic effects by conducting LB simulations on the exact geometries of the porous media in which imbibition and drainage experiments were performed. The LB model is of particular interest in that macro-scale dynamics of the multi-phase system are easily inferred from the collective behavior of pore-scale properties [Chen and Doolen, 1998]. In addition to the macro-scale mechanisms responsible for dynamic effects, there are underlying pore-scale properties that potentially contribute to dynamic effects. It has previously been hypothesized that the pore-scale mechanisms responsible for observed dynamic effects include velocity gradients created locally by the movement of a single meniscus [Vizika et al., 1994], air entrapment [Schultze et al., 1999], the presence of dynamic contact angles [Friedman, 1999] and water entrapment due to higher flow rates [Wildenschild et al., 2001], to name few. The pore-scale properties to be investigated in this study with the LB model include (1) the geometry of the pore space; (2) interfacial phenomena (i.e. interfacial tension, contact angle and interfacial area); and (3) the interaction between capillary and viscous forces. We hypothesize that during dynamic flow conditions the dominating pore-scale properties vary depending upon the location within the porous medium. This variation may, in drainage events, lead to areas at small pore throats where viscous forces dominate causing

relatively little decrease in local wetting phase due to a pressure build up at that pore throat. During the same drainage event, in larger pores, unstable curvatures may have formed, due to transient flow, that cause a significant decrease in local wetting phase, as well as, a decrease in local pressure.

A description of the LB method that supports this study is presented below. Due to the computational demands associated with LB methods, preliminary 2D simulations were completed. The 2D simulations serve to test the selected LB parameters and simulation conditions. The results in this manuscript primarily focus on these 2D simulations and their implications pertaining to dynamic effects.

3. LATTICE-BOLTZMANN SIMULATIONS

The LB model used in this study is a Shan and Chen [1993] type (hereafter, SC type model) multiphase and multi-component model as adapted by Martys and Chen [1996]. In the SC type model fluid-fluid and fluid-solid interaction potentials, as well as external body forces, are introduced in the macroscopic velocity that is used to update the particle distribution functions [Martys and Chen, 1996]. The reader is referred to Martys and Chen [1996] for a detailed description of the model. The D3Q19 and D2Q9 lattices are employed for 3D and 2D simulations, respectively. To simulate dynamic effects in a fashion that is consistent with the multi-step syringe pump experimental method (see Wildenschild et al. [1997] for details), flux boundary conditions (hereafter, referred to as flux) have been implemented at the inflow and outflow boundaries. Gravity forces have been ignored in the model since capillary and viscous forces dominate the systems in consideration. Pressure is calculated at each boundary and it is assumed that these pressure calculations are consistent with the experimental measurement of the fluid pressures outside the porous medium. Thus, it follows that the capillary pressure is the difference between the two pressures calculated at the boundaries.

4. RESULTS AND DISCUSSION

Results from various 2D multi-step drainage simulations are presented below. The lattice length scale (lu) and time step (ts) are taken as unity. Preliminary simulations were required to determine the interfacial tension between the two fluids, the fluid-solid interaction potential corresponding to a zero contact angle and equilibrium densities for initial conditions. These simulations consisted of phase separation and capillary tube simulations. The capillary tube simulations were conducted on different sized 2D capillary tubes in which a range of fluid-solid interaction potentials were tested. For details pertaining to these simulations see Schaap et al. [this proceeding]. From these results it was possible to choose an appropriate fluid-fluid and fluid-solid interaction potential, as well determine the interfacial tension. In all of the simulations presented here the kinematic viscosities are equal, thus the dynamic viscosity ratio, $M = \nu_0\rho_0/\nu_1\rho_1$ reduces to the density ratio, $M = \rho_0/\rho_1$. An average density ratio of approximately 1.0 or 0.79 was used in the simulations. The density ratio of 0.79 chosen here corresponds to the density ratio of Soltrol 220 and water, which are the fluids used in the macroscale oil/water experiments. For simulations in which $M = 1.0$ the interfacial tension was estimated as 0.165 $mu\ ts^{-2}$ (mass units per time step squared). For simulations in which $M = 0.79$ the interfacial tension was approximately 0.174 $mu\ ts^{-2}$.

The 2D porous media used in the following simulations were reconstructed using periodic overlapping spheres. The periodic porous media allows for implementation of the periodic boundary conditions for the sides of the domain. In Figure 1 the simulation domain is 128x145 lu and the percolating porosity is approximately 0.55. In al other simulations the domain is 256x275 lu and the percolating porosity is approximately 0.57. The porosities are large compared to real soils to ensure that at least one percolation path exists in the porous media. In order to calculate the pressure difference between the boundaries the fluids must be able to percolate from one end to the other.

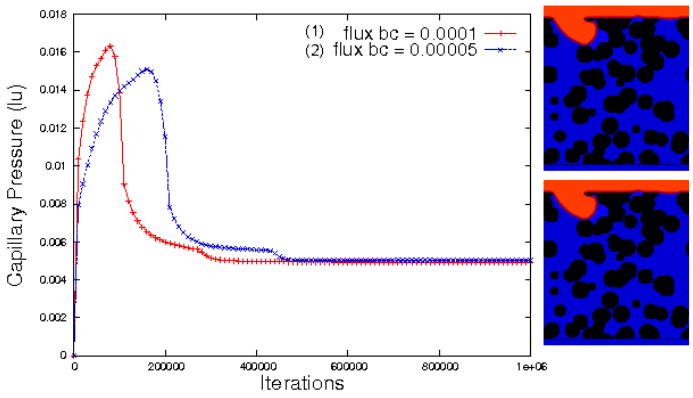

FIGURE 1. Capillary pressure for: (1) flux = 0.0001 $mu\ ts^{-1}$ for the the first 1e+05 ts, then flux = 0 $mu\ ts^{-1}$for the remainder of the simulation. The top image is the fluid configuration at 1e+06 ts. (2) flux = 0.00005 $mu\ ts^{-1}$ for the first 2e+05 ts, the flux = 0 $mu\ ts^{-1}$ for the remainder of the simulation. The bottom image is the fluid configuration at 1e+06 ts. $M = 1.0$ for both simulations.

Figure 1 shows results from two simulations that were designed to emulate the first step of a multi-step experiment with flux boundary conditions. The fluid mixture density ratio in these simulations is 1.0. The characteristic pore radius is 17.64 lu. In simulation (1) a flux = 0.0001 $mu\ ts^{-1}$ was imposed for 1e+05 ts followed by a flux = 0 $mu\ ts^{-1}$ to allow for equilibration. Similarly, in simulation (2) a flux = 0.00005 $mu\ ts^{-1}$ was imposed for 2e+05 ts followed by a flux = 0 $mu\ ts^{-1}$. At the times when the flux is set to zero the amount of non-wetting phase injected is nearly equal (It is not exactly equal due to density fluctuations inherent in LB models). The graph indicates that during transient flow and shortly after the flux is set to zero there are differences in the pressure profiles, however, the two simulations relax to almost identical capillary pressures and final fluid configurations after a sufficient number of iterations.

The graph in Figure 2 shows the capillary pressure results for four different simulations of the first step of a multi-step simulation with different fluxes and density ratios. In each simulation the flux is 0.0001 or 0.00005 $mu\ ts^{-1}$ for the first 1e+05 or 2e+05 ts, respectively, and then zero for the remainder of the simulation. The geometry of this porous media is considerably more complex than in Figure 1. The characteristic pore radius is 12.47 lu. The permeability for this porous media was estimated from single phase LB simulations to be 0.378 lu^2. When the density ratios are equal, the capillary pressures approach the same value despite the difference in the flux at early times. This is consistent with the results in Figure 1, and, based on simulations not presented here,

each of these simulations are nearing their respective equilibrium values (i.e. no more jumps are observed at later times).

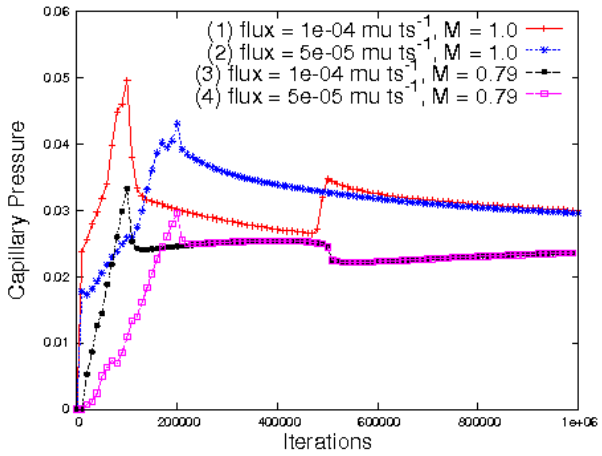

FIGURE 2. Capillary pressure for four different simulations with two density ratios and two flow rates. The capillary number for each simulation (1)-(4) is approximately 2.2e-04, 4.3e-04, 2.1e-04 and 4.3e-04, respectively.

The graph for simulation (1) in Figure 2 shows substantial movement of fluid well after the flux is set to zero. As the system relaxes it reaches a critical capillary pressure at which time a jump in the pressure occurs ($\simeq$ 4.7e+05 ts). The capillary pressure then continues to relax to a state of equilibrium, which it has not reached after 1e+06 ts. This indicates that equilibration time is highly dependent upon the geometry, which is consistent with experimental observations. The images in the first row of Figure 3 correspond to various fluid configurations prior to and following the pressure jump in simulation (1). A comparison of the image at 1e+05 ts and the image at 4.7e+05 ts indicates that a non-wetting phase finger forms in a pore after the flux was set to zero. The image at 5e+05 ts shows that this finger has moved back into the bulk of the non-wetting phase at the time the jump in pressure ends. The exact cause of this event has not been fully determined, however, one possible explanation is that the forces controlling the formation of the finger within the pore change while the system equilibrates. For instance, the pressure that built up at the pore throat while the flux was 0.0001 $mu\ ts^{-1}$ was larger than the non-wetting phase entry pressure, which lead to the formation of the finger, then as the capillary pressure decreased to a value less than the non-wetting phase entry pressure the finger quickly retreated back into the bulk of the non-wetting phase fluid due to capillary forces.

Comparing the simulations in which $M = 1.0$ (simulations (1) and (2) in Figure 2.) there is a large difference in capillary pressures for the two fluxes prior to approaching a similar state of equilibrium. The unstable finger (and, thus the pressure jump) that formed when the flux = 0.0001 $mu\ ts^{-1}$ does not form when the flux = 0.00005 $mu\ ts^{-1}$ (see Figure 3, first and second row). In the simulations where $M = 0.79$ the differences in capillary pressure due to the different fluxes at early times are minimal. The capillary pressures approach the same value and the pressure step to a lower capillary pressure

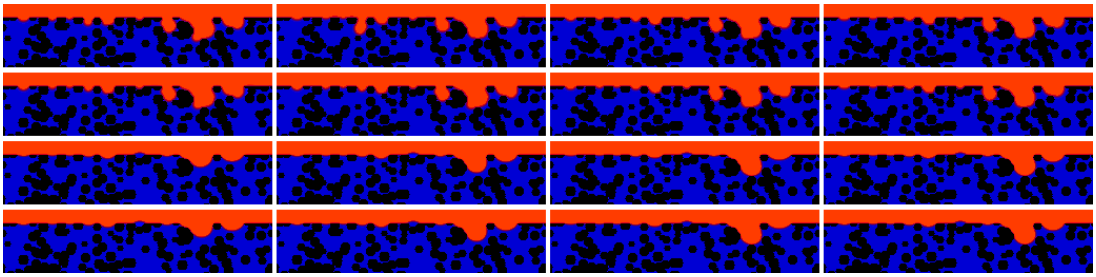

FIGURE 3. Fluid configurations at various *ts* for the simulations in Figure 2. The first row corresponds to 1e+05, 4.7e+05, 5e+05 and 1e+06 *ts* for simulation (1). The second row corresponds to 2e+05, 4.7e+05, 5e+05 and 1e+06 *ts* for simulation (2). The third row corresponds to to 1e+05, 4.8e+05, 5.1e+05 and 1e+06 *ts* for simulations (3). The fourth row corresponds to iteration 2e+05, 4.8e+05, 5.1e+05 and 1e+06 *ts* in simulation (4). The nonwetting phase is light gray and the wetting phase is dark gray

during equilibration are almost identical (see Figure 3 for fluid configurations near the step).

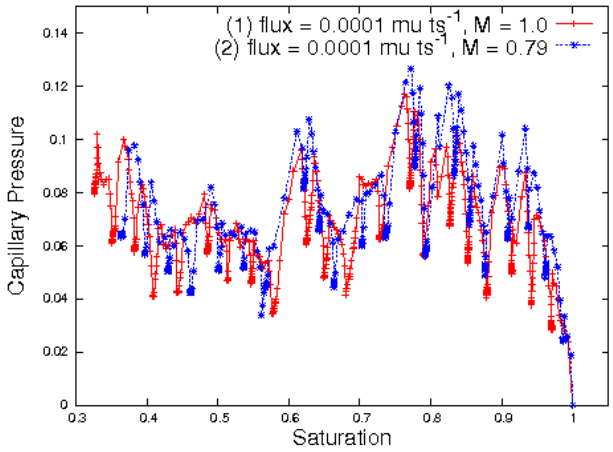

FIGURE 4. Capillary pressure vs. Saturation for two multi-step simulations with different density ratios.

Two different 2D multi-step drainage simulations were carried out in which only 2e+05 *ts* were allowed for equilibration, see Figure 4. The equilibration time was chosen such that the total simulation time was reasonable. In each case the flux was set to 0.0001 $mu\ ts^{-1}$ for 1e+05 *ts*, then set to zero to allow for the system to partially equilibrate. Although a state of equilibrium is not reached after each step, the simulations have the potential to provide insights, since it is often the case that equilibrium conditions are assumed for the experiments without knowing for certain equilibrium has been achieved. The pressures during transient flow have been included in the $P_c - S$ curve rather than just showing the quasi-static points. The results indicate that there is no monotonic trend in the capillary pressures as a function of the saturation (as is the case in the macroscale experiments). A comparison to the macroscale experiments is, however, premature because of the reduced connectivity in the 2D domain, an invasion percolation flow regime that led to many areas of trapped wetting phase (see Figure 5), the scale of the simulations and the increased density fluctuations due to the flux boundary conditions, to name a few. It should also be

noted that the capillary pressure in the simulations is estimated at the pore scale. In the macroscale experiments this is not the case. An interesting observation to note in Figure 4 is that the capillary pressure for a given saturation is generally greater for $M = 0.79$ than $M = 1.0$. This trend is especially evident at early times. This suggests that the less dense nonwetting phase fluid requires larger pressures to displace wetting phase fluid that is more dense. The fluid configurations at 6e+06 ts are presented for both simulations in Figure 5. The images indicate that the flow paths are indistinguishable except near the advancing nonwetting fluid front where the pressures at the pore throats required for nonwetting entry differ between simulations. The saturation for the images in Figure 5 are estimated to be in the range of 0.35-0.39. These images reaffirm that the lack of connectivity and the limited number of percolation paths in the porous media are the dominant controlling factors for the final fluid configurations in these simulations.

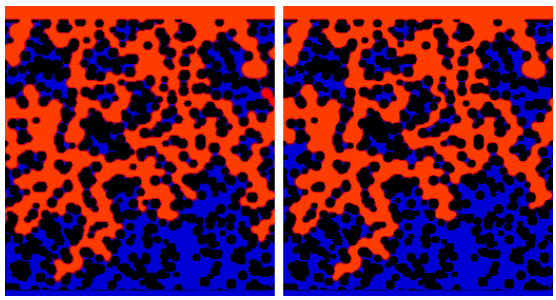

FIGURE 5. Fluid configurations at 6e+06 ts for two multi-step simulations. Left: $M = 1.0$. Right: $M = 0.79$. Light gray is nonwetting and dark gray gray is the wetting fluid.

5. CONCLUSIONS AND FUTURE WORK

Although limitations were encountered with LB simulations in 2D porous media, some interesting and useful information has been revealed that will need to be considered when conducting 3D simulations. The simulation of a single step revealed that often times a jump in the capillary pressure occurs relatively late in the equilibration process. Thus, a pressure profile that appears to be near equilibrium could actually be approaching a critical capillary pressure that will cause a rather significant reconfiguration leading to a very different equilibrium capillary pressure value. In a 3D porous medium in which the connectivity is greatly increased the magnitude of these pressure jump may not be as large, however, it is likely that similar jumps will be observed.

The multi-step simulations presented here were not carried out to a state of equilibrium for each step and they were not compared to a static $P_c - S$ curve, thus little can be said about dynamic effects observed in these simulations. The multi-step simulations did, however, indicate that the LB method shows promise in revealing the extent to which the density ratio contributes to dynamic effects.

The capillary pressure estimations in the 2D multi-step simulations were very noisy, which is of some concern. A number of factors could be contributing to this phenomenon. A likely cause is the density fluctuations in the fluid components. These density fluctuations are inherent in the LB method, however, the flux boundary conditions increase these fluctuations. Accounting for the density fluctuation quantitatively is difficult since

compressibility, unphysical density fluctuations near solid surfaces and small amount of diffusion between components at the interfaces all contribute to the fluctuations. It is expected that the transition to 3D porous media will reduce the magnitude of the density fluctuations.

It has been shown that LB model employed in this study is able to provide detailed information about the fluid configurations and pore scale phenomenon throughout 2D multi-step simulations. The next phase of the research is to investigate 3D multi-step and one-step (continuous flux) scenarios. Schaap et al. [this proceeding] has conducted preliminary 3D simulations of static $P_c - S$ with the same LB model using density boundary conditions. The 3D multi-step and one-step simulations will be compared with the static simulation results as well as, macro-scale experiments, and dynamic effects will be further investigated.

References

Bear, 1972. Bear, J. (1972). Dynamics of Fluids in Porous Media. Dover Publications Inc., New York. [Bear, 1972]

Bekri et al., 2001. Bekri, S. and P.M. Alder, 2001. Dispersion in multiphase flow through porous media. *International Journal of Multiphase Flow, 28*, 665-669.

Chen and Doolen, 1998. Chen, S. and G.D. Doolen, 1998. Lattice Boltzmann Method For Fluid Flows. *Annu. Rev. Fluid Mech. 30*, 329-364.

Davidson et al., 1966. Davidson, J.M., D.R. Nelson and J.W. Biggar (1966). The Dependence of Soil Water Uptake and Release Upon the Applied Pressure Increment. *Soil Science Society of America Proceedings, 30*, 298-304.

Friedman, 1999. Friedman,. S.P., 1999. Dynamic contact angle explanation of flow rate-dependent saturation-pressure relationships during transient liquid flow in unsaturated porous media. *J. Adhesion Sci. Technol., 13*(12), 1495-1518.

Hassanizadeh et al., 2002. Hassanizadeh, S.M., M.A. Celia, and H.K. Dahle, 2002. Dynamic Effect in the Capillary Pressure-Saturation Relationship and its Impacts on Unsaturated Flow. *Vadose Zone Journal, 1*, 38-57.

Li et al., 2005. Li, H., C. Pan and C.T. Miller, 2005. Pore-scale investigation of viscous coupling effects for two-phase flow in porous media *Physical Review E 72*,

Martys and Chen, 1996. Martys, N.S. and H. Chen, 1996. Simulation of multicomponent fluids in complex three-dimensional geometries by the lattice Boltzmann method. *Physical Review E, 53*(1), 743-750.

Muccino et al., 1998. Muccino, J.C., W.G. Gray and L.A Ferrand (1998). Toward an improved understanding of multiphase flow in porous media. *Reviews in Geophysics, 36*(3), 401-422.

O'Carroll et al., 2005. O'Carroll, D.M., T.J. Phelan and L.M. Abriola, 2005. Exploring dynamic effects in capillary pressure in multistep outflow experiments. *Water Resources Research, 41*(11).

Pan et al., 2004. Pan, C., M. Hilpert and C.T. Miller., 2004. Lattice-Boltzmann simulation of two-phase flow in porous media. *Water Resources Research, 40*(1).

Schaap et al., 2006. Schaap, M.G., B.S.B. Christensen, M.L. Porter and D. Wildenschild, 2006. Linking Experimental Capillary-Pressure Saturation Data with Lattice Boltzmann Simulations. *Presented at CMWR XVI - Computational Methods in Water Resources.* Copenhagen, Denmark, June, 2006.

Schultze et al., 1999. Schultze, B., O. Ippisch, B. Huwe and W. Durner, 1999. Dynamic Nonequilibrium During Unsaturated Water Flow. In: M. Th. Van Genuchten, F.j. Leij and L. Wu (ed.) *Proceedings of the Int. Workshop on Characterization and Measurement of the hydraulic Properties of Unsaturated Porous Media* Oct. 22-24, 1997. U. of California. Riverside CA.

Shan and Chen, 1993. Shan, X. and H. Chen, 1993. Lattice Boltzmann model for simulating flows with multiple phases and components. *Physical Review E, 47*(3), 1815-1819.

Shan and Doolen, 1996. Shan X. and G. Doolen, 1996. Diffusion in a multicomponent lattice Boltzmann equation model. *Physical Review E, 54*(4), 3614-3620.

Tölke et al., 2000. Tölke, J., M. Krafczyk, M. Schulz and E. Rank, 2000. Lattice Boltzmann simulations of binary fluid flow through porous media. *Phil. Trans. R. Soc. Lond. A, 360*, 535-545.

Topp et al., 1967. Topp, G.C., A. Klute and D.B. Peters, 1967. Comparison of water content-pressure head data obtained by equilibrium, steady-state and unsteady state methods. *Soil Sci. Soc. Am. J., 31*, 312-314.

Vizika et al., 1994. Vizika, O., D.G. Avraam and C. Payatakes, 1994. On the Role of the Viscosity Ratio during Low-Capillary-Number Forced Imbibition in Porous Media. *J. of Colloid and Interface Sci., 165*386-401.

Vogel et al., 2005. Vogel, H.-J., J. Tölke, M. Krafczyk, M. Schulz and K. Roth, 2005. Comparison of a Lattice-Boltzmann Model, Full-Morphology model, and a Pore Network Model for Determining Capillary Pressure-Saturation Relationships. *Vadose Zone Journal, 4*, 380-388.

Wildenschild et al., 1997. Wildenschild, D., K.H. Jensen, K.J. Hollenbeck, T.H. Illangasekare, D. Znidarcic, T. Sonneborg and M.B. Butts, 1997. A Two-Stage Procedure for Determining Unsaturated Hydraulic Characteristics using a Syringe Pump and Outflow Observations. *Soil Sci. Soc. Am. J., 61*, 347-359.

Wildenschild et al., 2001. Wildenschild, D., J.W. Hopmans and J. Simunek, 2001. Flow Rate Dependence of Soil Hydraulic Characteristics. *Soil Sci. Soc. Am. J., 65*, 35-48.